770 Gb/s PDM-32QAM Coherent Transmission Using InP Dual Polarization IQ Modulator

Mohammed Y.S. Sowailem, Thang M. Hoang, Mohamed Morsy-Osman, Mathieu Chagnon, Meng Qiu, Stéphane Paquet, Carl Paquet, Ian Woods, Qunbi Zhuge, Odile Liboiron-Ladouceur, *Senior Member, IEEE*, and David V. Plant, *Fellow, IEEE*

***Abstract*—We experimentally demonstrate 770 Gb/s (77 Gbd polarization division multiplexed 32QAM (PDM-32QAM)) transmission on a single wavelength using an Indium Phosphide (InP) dual polarization in-phase/quadrature (IQ) modulator over 320 km of standard single mode fiber (SSMF), which is suitable for low cost metro networks and datacenter interconnects (DCI). Moreover with the same setup we also demonstrate transmissions of 84 Gbd PDM-16QAM and 84 Gbd PDM-8QAM signals over 960 km and 1980 km distances, respectively, for regional and long-haul networks.**

***Index Terms*—Coherent Transmission System, Digital Signal Processing, Indium Phosphide Modulator, Modulation Formats.**

I. Introduction

Evolution of internet services such as online video streaming and cloud computing has tremendously increased network capacity demand, especially for datacenter interconnects (DCIs). 400 Gb/s coherent transceivers based on high symbol rates and spectrally efficient modulation formats are anticipated to be widely deployed soon for short distance DCI applications to satisfy their requirements for high capacity and low cost [1]. Recently, several demonstrations have been reported for high speed single carrier and OFDM technique transmissions [2-10]. For example, WDM transmission of 72 Gbd PDM-64QAM single carrier signals over 400 km of ultra large area fiber (ULAF) with hybrid Erbium doped fiber amplifier (EDFA)/Raman amplification at a bit error ratio (BER) of 3×10^{-2} was demonstrated in [2]. An optical filter was used to shape the spectrum to compensate for the limited bandwidth of the transmitter and a calibrated pre-distortion was done to mitigate inter-symbol interference (ISI).

Manuscript received December, 2016. This work is supported by Ciena, Corp.

Mohammed Y.S. Sowailem, Thang M. Hoang, Mohamed Morsy-Osman, Mathieu Chagnon, Meng Qiu, Odile Liboiron-Ladouceur, and David V. Plant are with ECE Department, McGill University, Montréal, QC H3A 2A7, Canada. (mohammed.sowailem@mail.mcgill.ca)

Mohamed Morsy-Osman is also with the EE Department, Alexandria University, Alexandria 21526, Egypt.

Stéphane Paquet, Carl Paquet, Ian Woods, and Qunbi Zhuge are with Ciena, Corp, Quebec City, QC G1P 4S8, Canada.

In parallel, the deployment of integrated photonics in DCIs to achieve cost-effective, pluggable and scalable coherent transceivers has captured many interests for manufacturers, researchers and designers [11-15]. The InP IQ modulator is a good candidate to realize integrated coherent transceivers with high 3-dB bandwidth at low values of V_π compared to other integrated solutions [15]. Also, it can be integrated monolithically with the laser source and the RF drivers. In [12], InP segmented Mach-Zehnder modulators (MZMs) were used to realize a single polarization IQ modulator with digital-to-analog converter (DAC)-free operation. Dual polarization emulation was done to demonstrate 32 Gbd PDM-64QAM transmission over 80 km at BER of 9.1×10^{-3}. In [16], we reported transmission of optical signal at payload rate of 400 Gb/s using a 2.5V V_π InP packaged dual-polarization IQ modulator (DP-IQM) with 35 GHz 3-dB bandwidth. This demonstration was enabled using a DAC operating at 65.7 GSps at the transmitter side and 33 GHz real time oscilloscope (RTO) operating at 80 GSps at the receiver side.

In this work, we further approach the bandwidth limit of the same InP DP-IQM and demonstrate up to payload rate of 600 Gb/s flexible transmissions as a cost-effective solution for next generation DCIs and backbone networks. In particular, we demonstrate various symbol rates and modulation formats including 77 Gbd PDM-32QAM (770 Gb/s), 84 Gbd PDM-16QAM (672 Gb/s), 84 Gbd PDM-8QAM (504 Gb/s), 84 Gbd PDM-QPSK (336 Gb/s), all enabled by a four-channel DAC operating at 84 GSps with 20 GHz 3-dB bandwidth that drives the InP DP-IQM at the transmitter and two RTOs operating at 160 GSps at the receiver. The maximum reach is 320 km, 960 km, 1980 km, and 4480 km for the four signals at a BER of 2×10^{-2}, respectively. The payload rate is about 600 Gb/s, 525 Gb/s, 400 Gb/s and 260 Gb/s, respectively, after the overall 28% overhead removal. Digital pre-emphasis is used to compensate for the transmitter limited bandwidth. A 4×4 real valued multiple-input-multiple-output (RV-MIMO) adaptive equalizer is used at the receiver for simultaneous polarization tracking and transceiver distortion mitigation instead of a 2×2 conventional complex MIMO (CC-MIMO) filter.

II. Experimental Setup and DSP Stack

A. Experimental Setup

Fig. 1 shows the experimental setup for our demonstration. Four AC-coupled 8-bit DACs operating at 84 GSps are used to

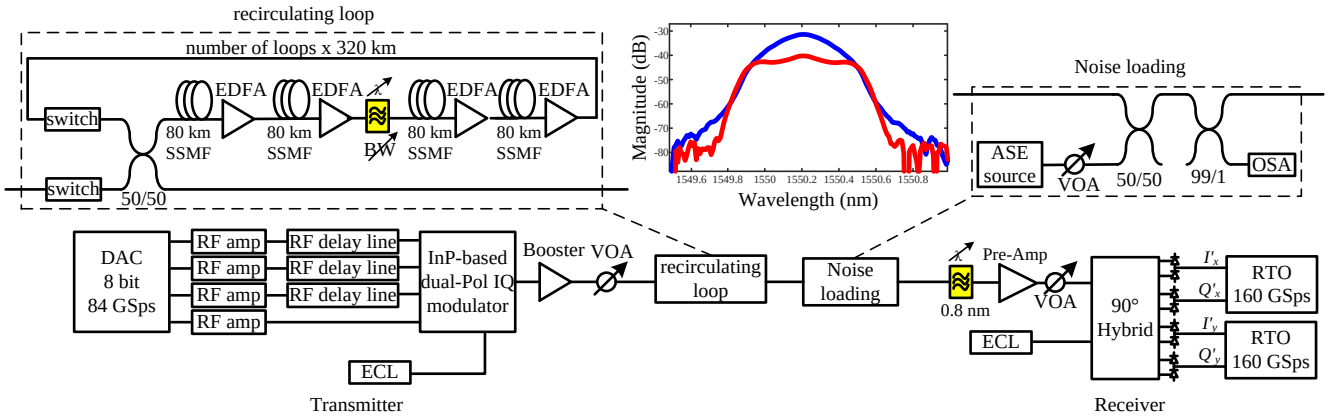

Fig. 1. Experimental setup. Inset: B2B optical spectrum with 0.05 nm resolution bandwidth for 84 Gbd signal with digital pre-emphasis (red curve) and without digital pre-emphasis (blue curve)

generate the four RF electrical signals, which are the base RF driving signals for optical modulation. The four RF electrical signals are then amplified by four discrete RF amplifiers with single-ended input and output, 50 GHz 3-dB bandwidth and a constant power gain of 26 dB with maximum output voltage of 8 $V_{pp.}$ The actual output swing from the RF amplifiers is around 1.9 $V_{pp.}$ at 84 Gbd and 2.2 $V_{pp.}$ at 77 Gbd. Next, RF delay lines (DC-63 GHz phase adjustable adaptors) are used to compensate for the skew between the four RF signals at the input of the DP-IQM due to RF cabling and other RF components. The DP-IQM is used for electro-optic conversion where the electric fields of two orthogonal polarizations of the continuous wave (CW) input light are optically modulated with the four RF signals. The CW light source is an external cavity laser (ECL) with 100 kHz linewidth operating at 1550.12 nm with an optical power of 15.5 dBm. The DP-IQM is a 2.5V V_{π} InP DP-IQM which has a 35 GHz 3-dB bandwidth, 10 dB insertion loss and less than 5 ps skew between X and Y polarization paths [16].

After electro-optic conversion, a booster EDFA is used to amplify the optical signal at a fixed average optical power of 23 dBm. Next, a variable optical attenuator (VOA) follows the booster to adjust the launched power of the signal to its optimum value for each modulation format and symbol rate. The signal is then launched into an optical re-circulating loop whose details are described in [16], which is used to achieve transmission distances that are integer multiples of 320 km. The re-circulating loop is followed by a noise loading block that is used for the purpose of optical-signal-to-noise-ratio (OSNR) measurements in the back-to-back (B2B) case. During the transmission measurements, the amplified spontaneous emission (ASE) noise source is blocked and it is enabled only during the OSNR measurements. The output of the noise loading block is connected to a 0.8 nm filter to remove the out of band noise followed by pre-amplifier and another VOA to optimize the received power. The optimized received power is found to be 6 dBm at the signal input port of the optical hybrid. Another ECL operating at 1550.12 nm is used as a local oscillator feeding the optical hybrid for coherent detection. The optical hybrid is followed by four balanced detectors with 40 GHz 3-dB bandwidth which are feeding two 62 GHz, 8-bit, RTOs operating at 160 GSps followed by offline signal processing.

B. DSP Stack

Fig. 2 illustrates the DSP stack used at the transmitter and receiver. The transmitter DSP (Tx-DSP) starts with N-QAM symbol generation for dual polarization transmission. The rest of the Tx-DSP depends on the operating symbol rate. At 84 Gbd which corresponds to operating the DAC at 1 sample per symbol, the generated symbols are pre-distorted by digital pre-emphasis followed by clipping and quantization processes. At 77 Gbd, the generated symbols are initially pulse shaped using a root-raised-cosine (RRC) filter at 2 samples per symbol with a roll-off factor of 0.09. Then re-sampling from 154 GSps to 84 GSps and digital pre-emphasis are applied on the data samples for equalization. Digital pre-emphasis is achieved using a finite-impulse-response (FIR) filter that is optimized experimentally to give minimum BER in the B2B case. The used number of taps for the FIR filter is 81 taps; however, 99% of the filter energy is concise in 15 taps only. Next, the equalized samples undergo non-linear compensation process to pre-invert the nonlinear transfer function of the MZMs of the DP-IQM and clipping procedure to minimize the peak-to-average-power-ratio. Finally, the samples are quantized and uploaded to the DAC memory.

The receiver DSP (Rx-DSP) is similar to the one in [16] except for timing recovery and polarization demultiplexing blocks. The timing recovery is done during the synchronization process for the captured data from both RTOs. For the polarization demultiplexing block, training symbol least mean squares (TS-LMS) and decision directed LMS (DD-LMS) are used for initial polarization tracking and steady state operation, respectively. However, we use a 4×4 RV-MIMO, similar to [17] and [18], instead of the 2×2 CC-MIMO for polarization tracking and adaptive filtering. The 2×2 CC-MIMO can be described employing Jones space representation of the signal as follows:

$$\begin{bmatrix} \boldsymbol{E_X^{out}} \\ \boldsymbol{E_Y^{out}} \end{bmatrix} = \begin{bmatrix} \boldsymbol{h_{xx}} & \boldsymbol{h_{xy}} \\ \boldsymbol{h_{yx}} & \boldsymbol{h_{yy}} \end{bmatrix} \begin{bmatrix} \boldsymbol{E_X^{in}} \\ \boldsymbol{E_Y^{in}} \end{bmatrix} \quad (1)$$

where, $\boldsymbol{E_X^{out}}$ and $\boldsymbol{E_Y^{out}}$ are the recovered complex electric fields after polarization tracking and adaptive filtering of the

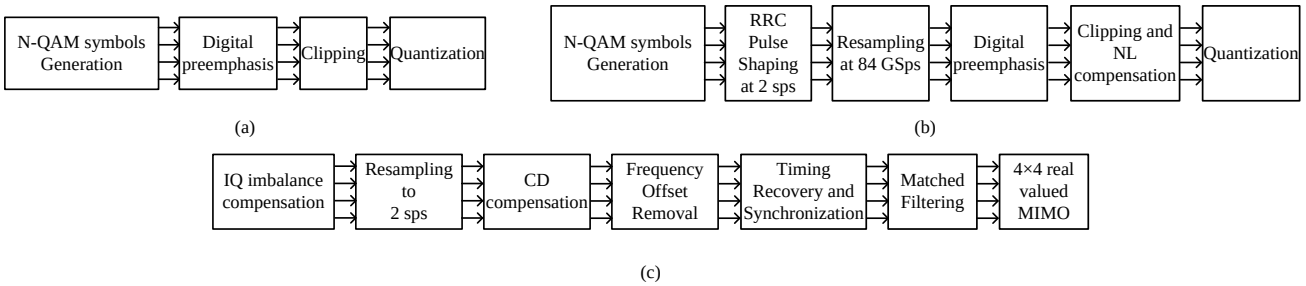

Fig. 2. DSP stack used for the transmission: (a) Tx-DSP for 84 Gbd at one sample per symbol (sps); (b) Tx-DSP for 77 Gbd; (c) Rx-DSP.

received complex electric fields $\boldsymbol{E_X^{in}}$ and $\boldsymbol{E_Y^{in}}$ using the filter taps $\boldsymbol{h_{xx}}, \boldsymbol{h_{xy}}, \boldsymbol{h_{yy}}$, and $\boldsymbol{h_{yx}}$. Similarly, the 4×4 RV-MIMO can be described by decomposing Eq. (1) into its real valued form and adjusting the real and imaginary parts of the filter taps to be independent as follows:

$$\begin{bmatrix} \boldsymbol{E_{X,I}^{out}} \\ \boldsymbol{E_{X,Q}^{out}} \\ \boldsymbol{E_{Y,I}^{out}} \\ \boldsymbol{E_{Y,Q}^{out}} \end{bmatrix} = \begin{bmatrix} \boldsymbol{h_{xx,ii}} & \boldsymbol{h_{xx,iq}} & \boldsymbol{h_{xy,ii}} & \boldsymbol{h_{xy,iq}} \\ \boldsymbol{h_{xx,qi}} & \boldsymbol{h_{xx,qq}} & \boldsymbol{h_{xy,qi}} & \boldsymbol{h_{xy,qq}} \\ \boldsymbol{h_{yx,ii}} & \boldsymbol{h_{yx,iq}} & \boldsymbol{h_{yy,ii}} & \boldsymbol{h_{yy,iq}} \\ \boldsymbol{h_{yx,qi}} & \boldsymbol{h_{yx,qq}} & \boldsymbol{h_{yy,qi}} & \boldsymbol{h_{yy,qq}} \end{bmatrix} \begin{bmatrix} \boldsymbol{E_{X,I}^{in}} \\ \boldsymbol{E_{X,Q}^{in}} \\ \boldsymbol{E_{Y,I}^{in}} \\ \boldsymbol{E_{Y,Q}^{in}} \end{bmatrix} \quad (2)$$

where, $\boldsymbol{h_{\theta\theta}}$ has been decomposed to $\boldsymbol{h_{\theta\theta,ii}}$, $\boldsymbol{h_{\theta\theta,iq}}$, $\boldsymbol{h_{\theta\theta,qq}}$, and $\boldsymbol{h_{\theta\theta,qi}}$ and $\boldsymbol{\theta\theta}$ can be any of $\boldsymbol{xx}$, $\boldsymbol{xy}$, $\boldsymbol{yx}$, and $\boldsymbol{yy}$. The computational complexity required for multiplications and additions of the RV-MIMO scheme is the same as the CC-MIMO, however, it requires more memory for storing the additional independent filter taps.

The advantage of using the 4×4 RV-MIMO over the 2×2 CC-MIMO in our setup is its higher ability to mitigate transmitter and receiver impairments namely: IQ imbalance and skew, which are significant impairments for high symbol rates with high order modulation formats. This ability is due to filtering both signal quadratures independently in case of the 4×4 RV-MIMO which allows the MIMO to correct any time skew or power imbalances between the two quadratures. It is worth noting that the 4×4 RV-MIMO was discussed before for compensating the receiver imperfections in [17] and [18]. However, it can be used to compensate for transmitter impairment especially for high speed systems that are sensitive to any residual IQ skew or imbalance. In [19], the authors investigated the impact of transmitter impairments on system performance introducing a DSP block to compensate for those impairments. This transmitter impairments compensation block included a 2×2 RV-MIMO applied on each polarization separately where polarization tracking is done prior to this DSP block. In our DSP stack, polarization tracking, carrier phase recovery and the IQ imbalance and skew compensation are combined in the 4×4 RV-MIMO.

III. Results

Fig. 3 shows the BER versus transmission distance using the 2×2 CC-MIMO and the 4×4 RV-MIMO for 77 Gbd PDM-32QAM and 84 Gbd PDM-16QAM, PDM-8QAM and PDM-QPSK signals at optimum launched power of ~3 dBm and received power of 6 dBm. In all cases, the 4×4 RV-MIMO provides better performance than the 2×2 CC-MIMO due to being more tolerant to residual IQ imbalance and IQ skew of the transceiver. These transceiver impairments can be attributed to the use of discrete electronic components between the DAC and the DP-IQM. For instance, in the 84 Gbd 16QAM case, the maximum reach at soft decision forward error correction threshold (SD-FEC) using 2×2 CC-MIMO is 640 km, while the maximum reach using 4×4 RV-MIMO is 960 km. As per Fig. 3, 77 Gbd PDM-32QAM, 84 Gbd PDM-16QAM and 84 Gbd PDM-8QAM signals are propagated and operated below SD-FEC at maximum distances of 320km, 960km and 1980 km, respectively. Also, the 84 Gbd PDM-QPSK signal is successfully transmitted over 2880 km, operating below the hard decision FEC threshold (HD-FEC) of 3.8 x 10^{-3}. Hence, a payload rate of 600 Gb/s single carrier transmission over 320 km of SMF is achieved using 77 Gbd PDM-32QAM modulation format at SD-FEC. Also, payload rates of 525 Gb/s and 390 Gb/s signals are transmitted at 84 Gbd over 960 km and 1920 km using 16 QAM and 8 QAM modulation formats, respectively, at SD-FEC. For 84 Gbd symbol rate QPSK modulation format, long haul transmission is achieved for payload rates of 300 Gb/s and 260 Gb/s over 2880 km and 4480 km at HD-FEC and SD-FEC, respectively.

Next, Fig. 4 shows the BER versus OSNR in 0.1 nm bandwidth measured by noise loading in B2B configuration for the 77 Gbd 32QAM, 84 Gbd 16QAM and 84 Gbd QPSK signals using the 4×4 RV-MIMO in the Rx-DSP. In addition, we plot the theoretical BER vs. OSNR curves corresponding to these symbol rates and modulation formats assuming additive white Gaussian noise (AWGN) channel. We also include in dotted lines the corresponding measured B2B BER floors taken from Fig. 3, i.e. when there is zero loaded ASE noise. Because of the presence of this noise floor, we conclude that by increasing the OSNR, the experimental BER-OSNR curves will converge to the B2B BER values that were achieved in absence of noise loading. These B2B BER floor values result mainly from the in-band electrical transmitter noise as discussed in [9], [16] and [20]. It can be noted that the 77 Gbd 32 QAM signal has ~7 dB implementation penalty at SD-FEC threshold which is higher than the implementation penalty (~5 dB) of the 84 Gbd 16QAM at SD-FEC despite the fact that the later has higher symbol rate. This is because the 32QAM signal requires more levels to represent the in-phase and quadrature electrical signals that are generated by the DACs compared to the 16 QAM signal. More specifically, higher order modulation formats require higher effective number of bits (ENOB) for the DACs since they are more sensitive to quantization noise due to the larger number of

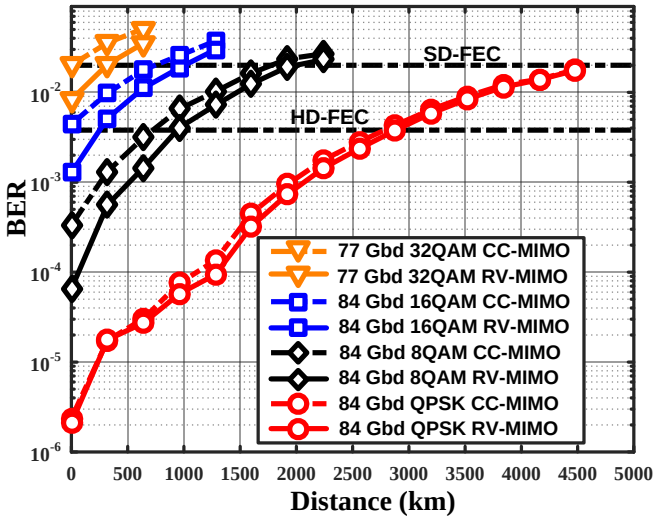

Fig. 3. BER versus distance for 77 Gbd PDM-32-QAM signal, 84 Gbd PDM-16QAM, PDM-8QAM and PDM-QPSK signals for two cases; using 2×2 CC-MIMO in Rx-DSP and using 4×4 RV-MIMO in Rx-DSP

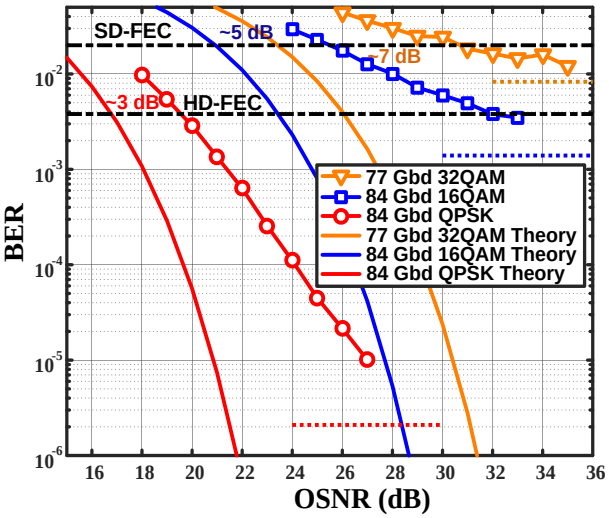

Fig. 4. BER versus OSNR for 77 Gbaud 32QAM signal, 84 Gbaud 16QAM and QPSK signals. Dotted lines represent B2B BER floors for each scenario which are taken from the BER curves at 0 km in Fig. 3.

required levels to represent the underlying drive signals. The same observation can be made for the 84 Gbd QPSK and 16QAM signals at HD-FEC. The QPSK signal which has the least ENOB requirement has ~3 dB implementation penalty at HD-FEC while the implementation penalty for the 16QAM signal is ~8.5 dB at HD-FEC.

IV. Conclusion

We demonstrated 770 Gb/s transmission using an InP DP-IQM on a single carrier including the required overhead at a symbol rate of 77 Gbd and PDM-32QAM modulation format over 320 km below SD-FEC. Also, transmissions are demonstrated at a symbol rate of 84 Gbd where bit rates of 504 Gb/s and 672 Gb/s are achieved using 8QAM and 16QAM modulation formats over 960 km and 1920 km, respectively below SD-FEC. Results show that the OSNR implementation penalty is highly dependent on the order of the modulation format due to its sensitivity to the transmitter noise. Finally, the viability of using InP DP-IQM is proved to meet up to payload rate of 600 Gb/s transmission system requirements for DCI applications.

References

[1] W. Idler, F. Buchali, and K. Schuh, "Experimental Study of Symbol-Rates and MQAM Formats for Single Carrier 400 Gb/s and Few Carrier 1 Tb/s Options," in *Proc. OFC 2016*, Anaheim, CA, 2016.

[2] S. Randel *et al*., "All-electronic flexibly programmable 864-Gb/s single-carrier PDM-64-QAM," in *Proc. OFC 2014*, San Francisco, CA, USA, 2014.

[3] F. Li *et al*., "82.29-Tb/s (182×560-Gb/s) Transmission of 42GHz-Spaced WDM PDM-128-QAM OFDM Signals over 100-km SMF," in *Proc. ECOC 2016*, Dusseldorf, Germany, 2016.

[4] Y. Fang *et al*., "Silicon IQ modulator based 480km 80×453.2Gb/s PDM-eOFDM transmission on 50GHz grid with SSMF and EDFA-only link," in *Proc. OFC 2015*, Los Angeles, CA, USA, 2015.

[5] F. Li *et al*., "Transmission of 8×520 Gb/s signal based on single band/λ PDM-16QAM-OFDM on a 75-GHz grid," in *Proc. OFC 2016*, Anaheim, CA, USA, 2016.

[6] X. Chen *et al*., "All-electronic 100-GHz Bandwidth Digital-to-Analog Converter Generating PAM Signals up to 190-GBaud," in Pro *OFC 2016*, Anaheim, CA, USA, 2016.

[7] G. Raybon, *et al.*, "Single-carrier 400G interface and 10-channel WDM transmission over 4800 km using all-ETDM 107-Gbaud PDM-QPSK," in *Proc. OFC 2013*, Anaheim, CA, USA, 2013.

[8] J. Zhang and J. Yu, "WDM Transmission of Twelve 960 Gb/s Channels based on 120-GBaud ETDM PDM-16QAM over 1200-km TeraWaveTM Fiber Link," in *Proc. OFC* , Anaheim, CA, USA, 2016.

[9] T. Rahman *et al*., "38.4Tb/s Transmission of Single-Carrier Serial Line-Rate 400Gb/s PM-64QAM over 328km for Metro and Data Center Interconnect Applications," in *Proc. OFC*, Anaheim, CA, USA, 2016.

[10] L. Dou, X. Su, Y. Fan, H. Chen, Y. Zhao, Z. Tao, T. Tanimura, T. Hoshida, and J. Rasmussen, "420Gbit/s DP-64QAM Nyquist-FDM single-carrier system," in *Proc. OFC 2016*, Anaheim, CA, USA, 2016.

[11] Y. A. Akulova, "Advances in Integrated Widely Tunable Coherent Transmitters," in *Proc. OFC 2016*, Anaheim, CA, USA, 2016.

[12] A. Aimone, I. Garcia Lopez, S. Alreesh, P. Rito, T. Brast, V. Höhns, G. Fiol, M. Gruner, J. Fischer, J. Honecker, A. Steffan, D. Kissinger, A. C. Ulusoy, and M. Schell, "DAC-free Ultra-Low-Power Dual-Polarization 64-QAM Transmission with InP IQ Segmented MZM Module," in *Proc. OFC 2016*, Anaheim, CA, USA, 2016.

[13] S. Chandrasekhar, X. Liu, P. Winzer, J. E. Simsarian and R. A. Griffin, "Compact all-InP laser-vector-modulator for generation and transmission of 100-Gb/s PDM-QPSK and 200-Gb/s PDM-16 QAM," *J. Lightw. Technol*, vol. 32, no. 4, pp.736 -742, 2014.

[14] V. Lal *et al*., "Full C-band tunable coherent transmitter and receiver InP photonic integrated circuits," in *Proc. ECOC*, Düsseldorf, Germany, Sep. 2016.

[15] Y. Ogiso *et al.*, "Ultra-High Bandwidth InP IQ Modulator with 1.5 V V_{π}," in *Proc. ECOC 2016*, Düsseldorf, Germany, Sep. 2016.

[16] M. Y.S. Sowailem, T. M. Hoang, M. Morsy-Osman, M. Chagnon, D. Patel, S. Paquet, C. Paquet, I. Woods, O. Liboiron-Ladouceur, and D. V. Plant, "400-G Single Carrier 500-km Transmission With an InP Dual Polarization IQ Modulator," *IEEE Photonics Technology Letters*, vol. 28, no. 11, pp. 1213-1216, June 2016.

[17] M. S. Faruk and K. Kikuchi, "Compensation for In-Phase/Quadrature Imbalance in Coherent-Receiver Front End for Optical Quadrature Amplitude Modulation," *IEEE Photonics Journal*, vol. 5, no. 2, pp. 7800110-7800110, April 2013.

[18] M. Paskov, D. Lavery and S. J. Savory, "Blind Equalization of Receiver In-Phase/Quadrature Skew in the Presence of Nyquist Filtering," *IEEE Photonics Technology Letters*, vol. 25, no. 24, pp. 2446-2449, Dec. 2013.

[19] Chris Fludger, and Theo Kupfer, "Transmitter Impairment Mitigation and Monitoring for High Baud-Rate, High Order Modulation Systems," in *Proc. ECOC 2016*, Düsseldorf, Germany, Sep. 2016.

[20] D. Rafique, A. Napoli, S. Calabro, and B. Spinnler, "Digital Preemphasis in Optical Communication Systems: On the DAC Requirements for Terabit Transmission Applications," *J. Lightw. Technol.*, vol.32, no.19, pp.3247-3256, Oct. 2014.